

CONDUCTION COOLING METHODS FOR Nb₃Sn SRF CAVITIES AND CRYOMODULES*

N. A. Stilin[†], A. Holic, M. Liepe, R. D. Porter, J. Sears, Z. Sun
Cornell Laboratory for Accelerator-Based Sciences and Education (CLASSE)
Ithaca, NY 14853, USA

Abstract

Rapid progress in the performance of Nb₃Sn SRF cavities during the last few years has made Nb₃Sn an energy efficient alternative to traditional Nb cavities, thereby initiating a fundamental shift in SRF technology. These Nb₃Sn cavities can operate at significantly higher temperatures than Nb cavities while simultaneously requiring less cooling power. This critical property enables the use of new, robust, turn-key style cryogenic cooling schemes based on conduction cooling with commercial cryocoolers. Cornell University has developed and tested a 2.6 GHz Nb₃Sn cavity assembly which utilizes such cooling methods. These tests have demonstrated stable RF operation at 10 MV/m and the measured thermal dynamics match what is found in numerical simulations.

INTRODUCTION

Studies conducted by the U.S. DOE and national labs have found that small-scale particle accelerators operating at a few MeV have the potential to be used in a wide range of applications spanning multiple industry fields. For example, particle beams can be used for producing imaging compounds in medicine, wastewater treatment for environmental progress, improved cargo scanning for national security, and many more [1, 2]. Currently, most small-scale industry operations are limited to the use of lower-efficiency cavities made of copper or other normal conducting materials. Although SRF technology offers significant improvements in cavity performance, the required use of liquid helium poses a significant barrier. Commercial cryocoolers have seen significant development in the last few years, but their cooling capacity of a couple Watts at 4 K is not enough for the operation of standard niobium SRF cavities.

Nb₃Sn-coated cavities provide the bridge to the use of cryocoolers in place of liquid helium. Nb₃Sn has a critical temperature of just over 18 K which allows for efficient cavity operation at temperatures of 4.2 K [3]. Steady improvements in the performance of Nb₃Sn cavities [3–9] have resulted in cavities capable of reliable operation at accelerating gradients relevant to the various applications described above. Therefore, if it can be shown that commercial cryocoolers

are capable of effectively cooling such cavities during regular RF operation, SRF technology will become more easily accessible to small-scale industry applications.

We would also like to acknowledge that both Fermi-Lab [10] and Jefferson Lab [11] have performed their own studies on conduction cooling setups with commercial cryocoolers. Those studies involved lower-frequency Nb₃Sn cavities operating at lower accelerating gradients.

ASSEMBLY

At Cornell University, we have designed and constructed a new testing assembly that is compatible with the use of a cryocooler. In our setup, we use a Cryomech PT420 cryocooler with the remote motor option. This model has two separate cooling stages, with the heat loads being dissipated at the corresponding cold heads. For optimal cooling conditions, the first cold head should dissipate 55 W of heat, which will result in a temperature of 45 K. In this case, the second cold head is capable of dissipating 1.8 W at 4.2 K [12]. The cooling capacity of the 2nd stage is slightly diminished if the 1st stage has a lower heat load. The remote option means that the primary exchange motor is isolated from the rest of the assembly. This was chosen to help reduce vibrations in the system, though it also slightly reduces the cooling capacity (from 2 W to 1.8 W for the 2nd stage). Figure 1 shows a slice-through of the 3D model for this testing assembly along with images of the primary cryocooler and exchange motor.

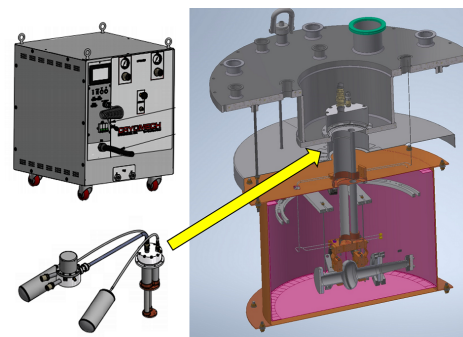


Figure 1: Overview of Cornell's cryocooler testing assembly. Top left: primary cryocooler unit (Cryomech PT420). Bottom left: cooling unit, comprised of the two cooling stages and remote exchange motor with helium gas reservoirs. Right: Inventor model of test assembly insert.

In our assembly, the 1st stage cold head is used to intercept most of the heat loads coming from room temperature via RF cables, wire connections, and so on. We have also attached

* This work was supported by the U.S. Department of Energy (DOE). U.S. DOE award DE-SC0008431 supports Nb₃Sn cavity coating and RF testing R&D, including the initial development of a conduction cooling assembly. U.S. DOE award DE-SC0021038 "Next Steps in the Development of Turn-Key SRF Technology" supports the full development of the conduction cooling concept.

[†] nas97@cornell.edu

a large copper thermal shield which surrounds the primary cavity assembly. This is done so that the cavity assembly is only exposed to radiation from 45 K rather than room temperature. In addition, both the thermal shield and the cavity assembly are covered with multi-layer aluminized mylar superinsulation to further reduce any heating from thermal radiation.

The 2nd stage cold head is reserved for cooling the primary cavity assembly. Since we are using a cryocooler setup, we need to construct an effective thermal pathway between the cavity equator region (where the most heat is generated) and the cryocooler cold head. The first portion of this path is made up of copper beam clamps which are attached to the cavity just outside the irises. To ensure better thermal contact, the beam tubes were first wrapped with rolled indium strips before attaching the beam clamps. The second portion of the thermal path is made up of six copper braided straps which connect the beam clamps to a copper block attached to the cold head. Four of the straps were made from oxygen-free high-purity copper (OFHC), while the remaining two were made in-house using electrolytic tough-pitch (ETP) copper. We used Apiezon N thermal grease at most contact areas in the assembly to further improve thermal contact. See Fig. 2 for a closer view of these components as shown in an ANSYS model.

ANSYS SIMULATIONS

Early stages of the design process were guided by the use of thermal simulations analyzed in ANSYS. These simulations focused on the primary cavity assembly as seen in Fig. 2. We used a few different thermal properties for the various copper components. The in-house ETP straps were set to RRR 50 copper, as ETP and RRR 50 copper have very similar thermal conductivity [13]. For the OFHC straps, an effective thermal conductivity was calculated in a separate ANSYS simulation using conduction values provided by the manufacturer. Finally, the remaining copper components used RRR 150, which was determined by resistivity measurements completed on an in-house sample. The thermal conductivity values for RRR 50 and RRR 150 copper came from standard NIST publications [14].

The example shown in Fig. 2 uses a heat load of 1 W in the cavity equator region. We set the 2nd stage cold head to a fixed temperature as determined by earlier cold head calibration tests. These tests involved attaching heaters directly to the 1st and 2nd stages and applying various heat loads. This allowed us to determine the temperature of the two cold heads as a function of the heat loads applied to each. The fundamental power coupler and its associated components are also included in the model, but we did not consider it a point of interest in the simulations.

This example shows that with 1 W of heat generated in the cavity, we find a roughly 1 K total thermal gradient between the cavity equator and 2nd stage cold head. The temperatures calculated are 4.46 K and 3.5 K, respectively. This total gradient is divided roughly equally between the two

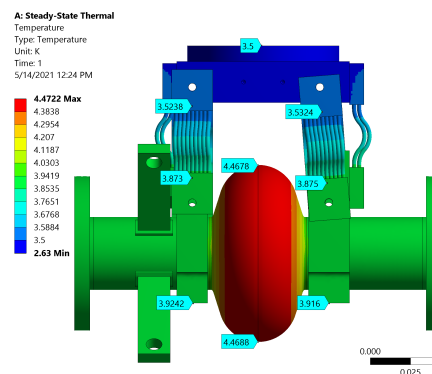


Figure 2: Numerical solution to thermal simulations run in ANSYS. Example shown uses a 1 W heat load dissipated in the cavity equator region. Notice that 80-85% of the temperature gradient between the cold head and beam clamps is concentrated at the copper braided straps.

main components of the thermal path: (1) from cold head to beam clamps (comprised of copper parts) and (2) from beam clamps to cavity equator (comprised of the Nb₃Sn-coated cavity). An important result we find in the simulations is that about 80-85% of the gradient between the 2nd stage cold head and beam clamps is concentrated at the copper braided straps. This indicates that an improvement to this portion of the thermal path could significantly improve the cooling capability in future studies involving cryocoolers.

CAVITY PERFORMANCE AND THERMAL BEHAVIOR

We now look at a comparison of various RF tests performed with the 2.6 GHz Nb₃Sn cavity used in this test assembly. See Fig. 3 for a combined plot comparing different QvE curves. As a baseline comparison, we include results from a 4.2 K standard vertical test which used liquid helium for cooling. In this test, the cavity reached a quench field of 17 MV/m with a low-field quality factor of about 8×10^9 [15]. The remaining tests fall into two sets, one set from a run of tests in January 2020 and another set from February 2021. The legend entries describe the cooling method preceding each respective RF test. The initial cooldown in each set is an uncontrolled cooldown starting at room temperature, usually taking about 24 hours to complete.

The first set of tests also includes “temperature cycles” at 20, 30, and 40 K. For these cycles, the cavity was allowed to warm up to the respective temperatures by turning off the cryocooler, at which point the cryocooler would be restarted and the assembly would cool back down. The “heater control” test in the second set describes another type of cycle in which heaters had been added to each of the beam clamps. This allowed us to add high enough heat loads to the assembly to warm up the cavity above 18 K while leaving the cryocooler on. In this process, we were able to balance the temperatures between the two clamps to within 5 mK of each other while the cavity slowly cooled back down through T_c.

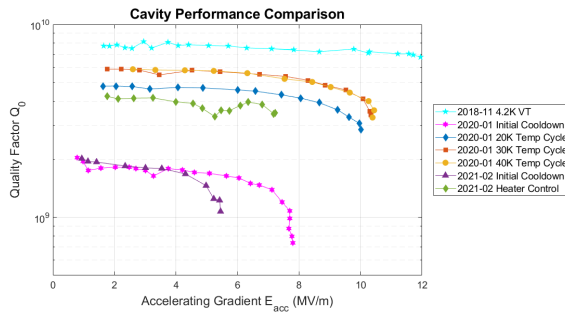


Figure 3: Comparison of various QvE curves for the 2.6 GHz Nb_3Sn cavity used in this study. We see poor performance following an initial cooldown, which is improved by better-controlled cooldown methods.

As seen in Fig. 3, we find significant differences in cavity performance based on what cooling method preceded each RF test. Both initial cooldown tests see relatively poor performance with a low-field quality factor of only about 2×10^9 . The temperature cycle tests and heater control tests all resulted in noticeable improvement, increasing the low-field quality factor to $4\text{--}6 \times 10^9$. It is interesting to note that the heater control test saw worse cavity performance than the temperature cycle tests, even though the temperature gradient between the two beam clamps was much smaller while cooling down the cavity. The temperature cycles had gradients of approximately 100 mK or higher, while the heater control cooldown maintained a gradient of less than 5 mK. This indicates that there may have been some form of cavity degradation between these sets of tests, though the exact cause of this is not clear.

In addition to the quality factor, we see significant differences in the maximum accelerating gradient reached between different tests. While the initial cooldown test from the 2020 set only reached about 8 MV/m, each of the subsequent temperature cycle tests reached an accelerating gradient of 10 MV/m. This would correspond to a beam energy gain of roughly 0.5 MeV for a 2.6 GHz cavity. Looking at the tests from 2021, we see a noticeable reduction in maximum accelerating gradient. The initial cooldown test reached just over 5 MV/m while the heater control test only reached about 7 MV/m. This may indicate the presence of higher static heat loads in the more recent test cycle, which would reduce the effective cooling capability of the 2nd stage cold head.

To better understand some of the cooling dynamics, we can look at the thermal behavior of the cavity assembly measured in some of the RF tests. In order to monitor the assembly, we placed Cernox temperature sensors on the 2nd stage cold head, both beam clamps, and the cavity equator. Figure 4 shows a comparison of these temperatures between the 30 K temperature cycle test and the heater cycle test. We can see that the cavity assembly both starts at a higher temperature and heats up faster in the heater control test. The higher starting temperatures again suggest a higher static heat load, while the faster heating indicates worse cavity quality factor, which again could be due to cavity degrada-

tion. An interesting feature to notice is that the assembly temperatures are roughly the same at the maximum accelerating gradient in each respective test. This suggests that beyond these temperatures we see thermal runaway, in which the cooling capability of the cryocooler can no longer keep up with the warming from the cavity. In this case, any additional power put into the cavity only leads to further heating rather than producing increased accelerating fields.

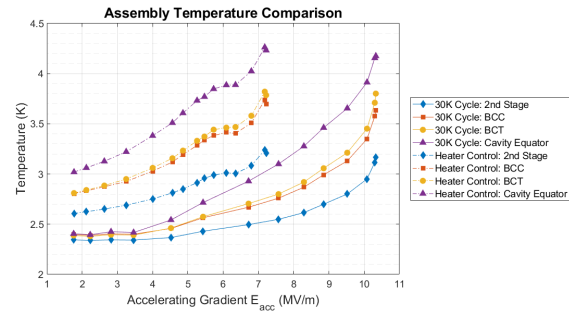


Figure 4: Comparison of the cavity assembly temperatures between the 30 K temperature cycle test and the heater control test. BCC and BCT correspond to the beam clamp on the coupler side and the beam clamp on the furnace tab side of the cavity cell, respectively.

CONCLUSION

At Cornell University, we have developed a new cryocooler testing assembly which utilizes a 2.6 GHz Nb_3Sn cavity to examine the effectiveness of cryocoolers as a cooling method for SRF operation. Through various sets of RF tests, we have found that commercial cryocoolers indeed provide a viable alternative to liquid helium when using Nb_3Sn -coated cavities. With our test assembly, we were able to successfully operate a 2.6 GHz Nb_3Sn cavity at 10 MV/m. By comparing cavity performance between different sets of tests, we found clear indications that minimizing static heat loads is crucial for maximizing cavity quality factor and attainable accelerating gradients, as larger static loads reduce the cryocooler's effective cooling capabilities.

By comparing RF results within a given set of tests, we found that different cooling methods can improve cavity performance. These better cooling methods all resulted in lower thermal gradients across the cavity as it cooled through T_c , indicating that reducing these gradients is a key factor in increasing RF performance. This matches what we might expect from an understanding of the thermoelectric effect. Temperature gradients present during cooldown generate thermoelectric currents in the bi-metal structure of Nb and Nb_3Sn . These currents generate magnetic fields which can get trapped in the cavity and increase RF dissipation [16].

As the next step in our studies, we plan to begin the design and development of a standalone SRF cryomodule which operates using two commercial cryocoolers. This cryomodule will contain a 1.3 GHz Nb_3Sn cavity with an input coupler capable of delivering high beam current.

REFERENCES

- [1] U. S. DOE Report, “Accelerators for America’s Future”, U.S. Department of Energy, Washington: High Energy Physics, Jun. 2010.
- [2] U. S. DOE Report, “Workshop on Energy and Environmental Applications of Accelerators”, ANL, Argonne, Illinois, USA, Jun. 2015.
- [3] S. Posen and M. Liepe, “Advances in development of Nb₃Sn superconducting radio-frequency cavities”, *Phys. Rev. ST Accel. Beams*, vol. 17, p. 112001, Nov. 2014. doi:10.1103/PhysRevSTAB.17.112001
- [4] S. Posen, “Understanding and Overcoming Limitation Mechanisms in Nb₃Sn Superconducting RF Cavities”, Ph.D. thesis, Phys. Dept., Cornell University, Ithaca, NY, USA, 2014.
- [5] D. L. Hall, “New Insights into the Limitations on the Efficiency and Achievable Gradients in Nb₃Sn SRF Cavities”, Ph.D. thesis, Phys. Dept., Cornell University, Ithaca, NY, USA, 2017.
- [6] S. Posen, M. Liepe, and D. L. Hall, “Proof-of-principle demonstration of Nb₃Sn superconducting radiofrequency cavities for high Q₀ applications”, *App. Phys. Lett.*, vol. 106, p. 082601, 2015. doi:10.1063/1.4913247
- [7] S. Posen and D. L. Hall, “Nb₃Sn Superconduction Radiofrequency Cavities: Fabrication, Results, Properties, and Prospects”, *Supercond. Sci. Technol.*, vol. 30, no. 3, p. 33004, Jan. 2017. doi:10.1088/1361-6668/30/3/033004
- [8] S. Posen *et al.*, “Advances in Nb₃Sn superconducting radiofrequency cavities towards first practical accelerator applications”, *Supercond. Sci. Technol.*, vol. 34, no. 2, p. 025007, Jan. 2021. doi:10.1088/1361-6668/abc7f7
- [9] U. Pudasaini *et al.*, “Recent Results From Nb Sn Single Cell Cavities Coated at Jefferson Lab”, in *Proc. 19th Int. Conf. RF Superconductivity (SRF’19)*, Dresden, Germany, Jun.-Jul. 2019, pp. 65–70. doi:10.18429/JACoW-SRF2019-MOP018
- [10] R. C. Dhuley, S. Posen, M. I. Geelhoed, O. Prokofiev, and J. C. T. Thangaraj, “First demonstration of a cryocooler conduction cooled superconducting radiofrequency cavity operating at practical cw accelerating gradients”, *Supercond. Sci. Technol.*, vol. 33, no. 6 p. 06LT01, Apr. 2020. doi:10.1088/1361-6668/ab82f0
- [11] G. Ciovati, G. Chen, U. Pudasaini, and R. A. Rimmer, “Multi-metallic conduction cooled superconducting radio-frequency cavity with high thermal stability”, *Supercond. Sci. Technol.*, vol. 33, no. 7 p. 07LT01, May 2020. doi:10.1088/1361-6668/ab8d98
- [12] Cryomech, <https://www.cryomech.com/products/pt420/>.
- [13] J. Ekin, *Experimental Techniques for Low-Temperature Measurements*, Oxford, United Kingdom: Oxford University Press, 2006.
- [14] P. Bradley and R. Radebaugh, *Properties of Selected Materials at Cryogenic Temperatures*, Boca Raton, FL, USA: CRC Press, 2013.
- [15] R. D. Porter, M. Liepe, and J. T. Maniscalco, “High Frequency Nb Sn Cavities”, in *Proc. 19th Int. Conf. RF Superconductivity (SRF’19)*, Dresden, Germany, Jun.-Jul. 2019, pp. 44–47. doi:10.18429/JACoW-SRF2019-MOP011
- [16] D. L. Hall, M. Liepe, R. D. Porter, D. Liarte, and J. P. Sethna, “Field-dependence of the Sensitivity to Trapped Flux in Nb₃Sn”, in *Proc. 18th Int. Conf. RF Superconductivity (SRF’17)*, Lanzhou, China, Jul. 2017, pp. 844–847. doi:10.18429/JACoW-SRF2017-THPB042